Proceedings of The Joint Canadian Society for Mechanical Engineering and CFD Society of Canada International Congress 2019
CSME-CFDSC Congress 2019
June 2-5, 2019, London, On, Canada

AIRFLOWS IN NARROW STREET CANYONS: SINGLE OR DOUBLE VORTEX?

Lup Wai Chew
Department of Mechanical Engineering
Massachusetts Institute of Technology
Cambridge, MA, USA
lupwai@mit.edu

Amir A. Aliabadi
Environmental Engineering Program
University of Guelph
Guelph, ON, Canada
aaliabad@uoguelph.ca

Leslie K. Norford
Department of Architecture
Massachusetts Institute of Technology
Cambridge, MA, USA
lnorford@mit.edu

Abstract—Airflows in narrow urban street canyons (canyons with height-to-width aspect ratio of 2.0 or higher) are generally understood to induce two counter-rotating vortices. We show that the double-vortex regime only exists at low Reynolds numbers, *Re* (~10^4). At high *Re* (~10^5 or higher), only one vortex is observed, consistent with full-scale field measurement at *Re* ~10^6. The change from double-vortex regime at relatively low *Re* to the single-vortex regime at high *Re* suggests that the widely adopted critical *Re* (where $Re \geq$ 10,000 is sufficiently high to ensure *Re*-independent flow) is not applicable for narrow street canyons.

Keywords - CFD simulations; high aspect ratio canyon; Reynolds number independence; skimming flow

I. INTRODUCTION

Airflows across urban areas have been studied extensively, as they have direct impacts on many aspects of built environments. For example, architectural features such as roof shape and building porosity can channel more winds into urban areas to enhance pollutant dispersion and improve the air quality [1–4]. Britter and Hanna [5] categorized the study of urban airflows into four scales: regional (~100 km), city (~10 km), neighborhood (~1 km), and street (~0.1 km). This paper focuses on the street scale, where we can resolve the flow features in individual urban street canyons. Urban street canyons ("canyons" hereafter) are outdoor spaces between buildings. When the street length is much larger than the building height, a two-dimensional (2D) canyon is formed. Under perpendicular winds, 2D canyons with a height-to-width aspect ratio (*H*/*W*) larger than 0.7 exhibit the skimming flow pattern [6], which is the most severe in terms of pollutant or heat trapping inside canyons [5,7]. Therefore, many studies have investigated the skimming flow regime in 2D canyons.

TABLE I. SUMMARY OF STUDIES ARRANGED BY CANYON ASPECT RATIO (H/W) AND REYNOLDS NUMBER (RE).

No.	Authors	H (m)	W (m)	H/W	Re	No. of vortices
1	Caton et al. [8]	0.07	0.07	1.0	3,000	1
2	Gerdes & Olivari [9]	0.03	0.03	1.0	4,000	1
3	Baik et al. [10]	0.24	0.24	1.0	10,000	1
4	Li et al. [11]	0.1	0.1	1.0	12,000	1
5	Kovar-Panskus et al. [12]	0.29	0.29	1.0	19,000	1
6	Meroney at al. [13]	0.06	0.06	1.0	20,000	1
7	Brown et al. [14]	0.15	0.15	1.0	30,000	1
8	Nakamura & Oke [15]	17.0	16.0	1.06	2.1×10^6	1
9	Baik et al. [10]	0.24	0.12	2.0	10,000	2
10	Li et al. [11]	0.1	0.05	2.0	12,000	2
11	Eliasson et al. [16]	15.0	7.1	2.1	1.9×10^6	1
12	Santamouris et al. [17]	20.0	8.5	2.35	2.5×10^6	1

Table I lists selected experiments and field studies with *H*/*W* between 1.0 and 2.4. Note that the height of canyons could be as small as 0.03 m (in reduced-scale experiments) and as large as 37 m (in full-scale field measurements). The Reynolds number, $Re = HU_{ref}/\nu$, is a dimensionless parameter to compare the scale, where U_{ref} is a reference wind speed (often taken to be the freestream wind speed), *H* is building height, and ν is the kinematic viscosity. Reduced-scale

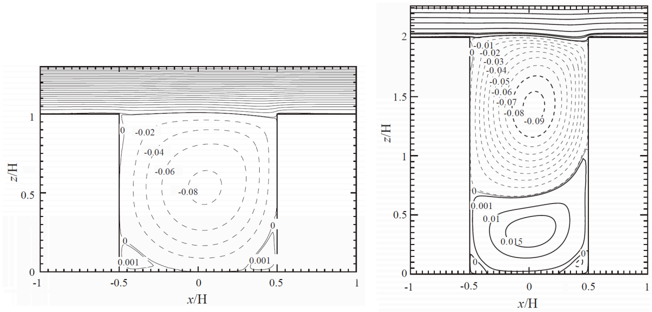

Fig. 2. Contours of stream-functions at Reynolds number 12,000. Left: flow across a canyon with $H/W = 1.0$, where a single vortex is observed (excluding the minor corner vortices). Right: flow across a canyon with $H/W = 2.0$, where two counter-rotating vortices are observed. Images from Li et al. [18].

experiments have *Re* on the order of 10^3 to 10^4, while full-scale field measurements have *Re* two orders of magnitude higher at 10^6. At *Re* $\sim 10^4$, a single quasi-steady vortex is induced in a canyon with $H/W = 1.0$. In a narrow canyon, where $H/W = 2.0$, two vortices could be induced, as shown in Fig. 1 [18].

The *Re* required for *Re*-independent flows is often taken to be 10,000 [10,11,13,19]. This means that the flow pattern does not change with increasing *Re* when *Re* exceeds 10,000. Studies 1-8 in Table I show that increasing the *Re* from 3,000 to 30,000, and further to 10^6, does not change the number of vortices in canyons with $H/W = 1.0$ (all studies reported one vortex). This means that the effect of *Re* is negligible, or the flows are *Re*-independent. However, this is not true for canyons with $H/W = 2.0$. Studies 9 and 10 in Table I reported two vortices at *Re* ~10,000, but studies 11 and 12 reported only one vortex at *Re* $\sim 10^6$. Clearly, the flows are not *Re*-independent in this range of *Re*, since the flow pattern changes when the *Re* is increased above 10,000. Our previous experimental work has shown evidence that *Re*-independence is achieved at *Re* ~70,000 for canyons with $H/W = 2.0$ [20]. However, only the velocity profiles were measured and no flow visualization is performed. This paper extends the study numerically by conducting computational fluid dynamics (CFD) simulations to visualize the overall flow fields in the canyons at different *Re*.

II. Numerical Model

A. *Description of Simulation Setup*

Fig. 2 shows the 2D CFD domain. The dimension of the buildings and canyon follow those in our water channel experiments [20], which are used for model validation. The canyon height is $H = 0.2$ m while the canyon width is $0.5H$. Both the upstream and downstream buildings have a width of $0.6H$. Since a periodic boundary is employed on the left and right boundaries, the building width is halved to $0.3H$ in the CFD model. The top of the surface is 2.75H from the ground to match the water depth in the experiments. The top surface is a free-slip wall. The roof, walls, and ground have a no-slip boundary condition. The left and right boundaries have a periodic boundary condition, meaning that the domain repeats itself in the streamwise direction, forming an array with an infinite number of canyons. The initial conditions are zero for all parameters, except for the streamwise velocity, where a freestream velocity is prescribed based on the *Re* in each simulation.

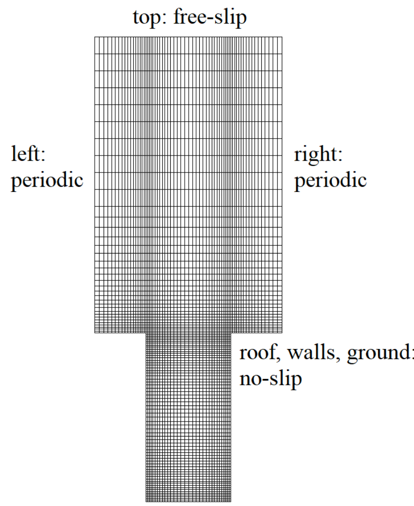

Fig. 1. Mesh and boundary conditions of the simulation domain

The model is built and meshed in the ANSYS workbench package version R17.2. All grids are perfectly orthogonal (hexahedral). The grids near the walls are refined. The maximum grid expansion ratio is 1.2. The simulations are run with ANSYS FLUENT. A steady Reynolds-Averaged Navier-Stokes (RANS) solver with the standard k-epsilon turbulence closure scheme is used. We repeat the simulations with realizable and RNG k-epsilon schemes and obtain identical results. The enhanced wall treatment is selected based on the recommendation for wall-resolving flows [21]. The SIMPLEC (Semi-Implicit Method for Pressure-Linked Equations-Consistent) algorithm is used for pressure-velocity coupling. For discretization, the Least Squares Cell Based method is used for gradients and the second order scheme is used for all other parameters. The convergence criterion is set at 10^{-5} for all variables, which is achieved after 10,000 iterations. To test for convergence, the simulation is continued for another 10,000 iterations. The results do not change, confirming that a converged solution has been obtained.

B. *Mesh Independence Study*

Three models with coarse, normal, and fine mesh resolutions are built for mesh sensitivity study. The numbers of grids are 4,358, 17,572, and 39,432, respectively. For brevity, only the coarse mesh model is shown in Fig. 2. Fig. 3 compares the normalized streamwise velocity profiles at the middle of the canyon. The vertical distance from the ground, z, is normalized by the canyon height, H, while the streamwise velocity, u, is normalized by the freestream velocity, U_{ref}. The *Re* is 105,000, and the initial and boundary conditions are identical for all three models. The profiles from all three models have negligible difference above $z/H = 0.2$. Near the ground level (z/H between 0 and 0.2), the coarse mesh model underpredicts the u/U_{ref} magnitude. The normal mesh model produces a profile identical to that of the fine mesh model, confirming that the normal mesh resolution is sufficiently fine. However, to achieve a dimensionless wall distance (y^+) on the order of 1, the fine mesh model is used for all subsequent simulations.

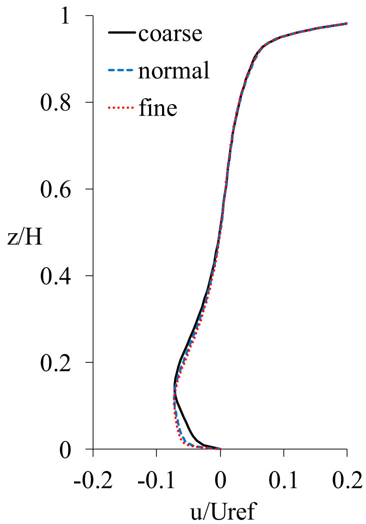

Fig. 3. Comparison of the normalized streamwise velocity profiles from the three models with different mesh resolutions.

C. Model Validation

The water channel experiments in [20] are used for CFD model validation. The detailed experimental setup and methodology is available in [22]. The *Re* range is between 12,000 to 105,000 in the experiments. We conduct CFD simulations for each *Re* and compare the simulation results to the experiments. Fig. 4 shows that the simulated u/U_{ref} profiles agree well with the experiments. At the lowest *Re* (12,000), the CFD model correctly predicts the low velocity region at the bottom half of the canyon ($z/H < 0.5$). At the highest *Re* (105,000), the CFD model also correctly predicts the negative velocity near the ground level. The fractional bias, FB = $2\ \overline{(u_s - u_e)}\ /\ (\overline{u_s} + \overline{u_e})$, and the normalized mean-square error, NMSE = $\overline{(u_s - u_e)^2}\ /\ (\overline{u_s} \times \overline{u_e})$ are used to quantify the errors [23]. The over-bar represents average (the spatial average of the line profile in this study), u is the velocity, subscript s represents simulation, and subscript e represents experiment. The FB for each case (*Re* of 12,000, 28,000, 57,000, 87,000, and 105,000) is -0.033, 0.017, 0.058, 0.050, and 0.055, respectively. The NMSE is 0.016, 0.019, 0.025, 0.025, and 0.031, respectively. Since the FB and NMSE for all cases are small, the CFD models are considered validated.

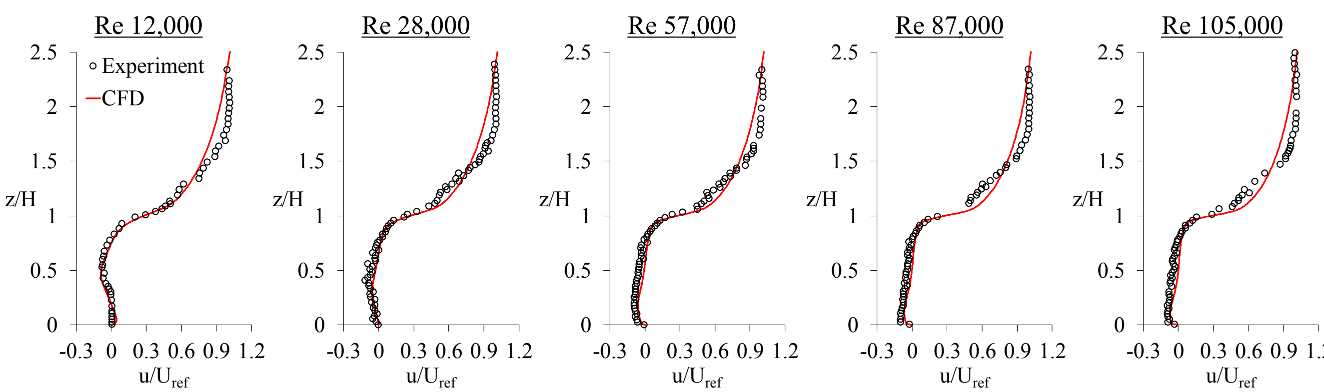

Fig. 4. Comparison of simulated streamwise velocity profiles to experiments at different Reynolds number. All profiles taken at the middle of the canyon.

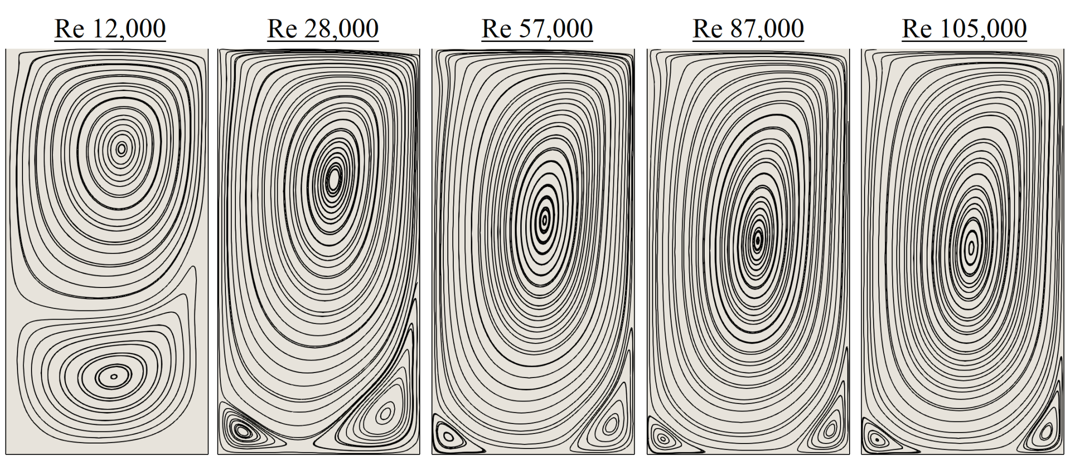

Fig. 5. Streamlines at different Reynolds number. When the Reynolds number is increased, the top vortex grows and the bottom vortex shrinks.

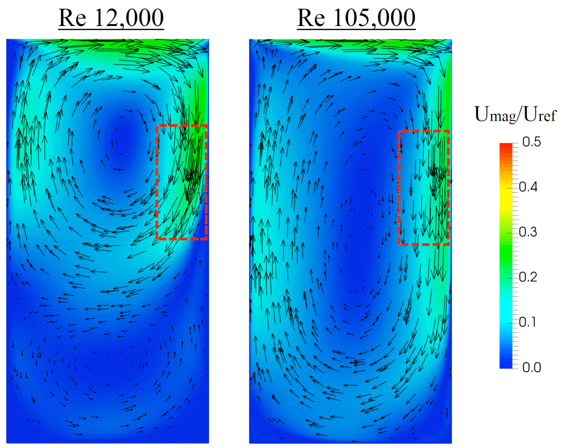

Fig. 6. Contours and vector plots of normalized velocity magnitude. At *Re* 12,000, the downward flow along the windward wall loses its vertical momentum near the mid-canyon height, as indicated by the red box. In contrast, at *Re* 105,000, the downward flow continues to flow along the windward wall.

III. Results and Discussion

The experiments provide only the line velocity profiles but not the full flow fields. The (validated) CFD models complement this drawback by providing visualization of the whole flow fields in the canyons. Fig. 5 compares the streamlines at different *Re*. At *Re* of 12,000, the double-vortex flow regime is obtained, similar to the results in the literature [10,11]. When the *Re* is increased to 28,000, the top vortex grows and occupies a larger region in the canyon, while the bottom vortex shrinks. The top vortex grows even larger when the *Re* is further increased to 57,000, while the bottom vortex breaks into two corner vortices. Increasing the *Re* from 57,000 to 87,000 and further to 105,000 does not result in significant changes in the flow pattern.

Why does *Re* affect the number of vortices in a canyon? Referring to Fig. 6, the shear layer at the building height induces a downward velocity near the windward wall of the building (the wall facing the incoming wind). This downward velocity indicated in the red box is about $0.3U_{ref}$. In other words, the local *Re* is about 30% of the global *Re*, i.e., the local *Re* is 3,600 and 31,500 for the cases with *Re* 12,000 and *Re* 105,000, respectively. For the case with a higher local *Re*, this downward velocity penetrates deeper into the canyon and creates only one major vortex inside the canyon. With higher *Re*, the entire regime (energy-containing, inertial subrange, and dissipation range) in the turbulence kinetic energy cascade shifts. It is speculated that the double-vortex pattern, which is caused by viscous dissipation at relatively low *Re*, does not form at high *Re*. In fact, at high *Re*, the inertial subrange, which is driven only by inertia-dominated dissipation, is extended to cover scales of motion close to the canyon length scale. In this range, viscous dissipation is negligible compared to the inertia-dominated dissipation of turbulence kinetic energy [24]. This explains why only one vortex forms at relatively high *Re*.

To summarize, Fig. 5 shows that the commonly adopted critical *Re* = 10,000 for *Re*-independent flows does not hold in canyons with aspect ratio 2.0. Many reduced-scale studies have reported the double-vortex flow pattern in narrow street canyons and generalized the results to full-scale canyons. Consequently, applications derived based on the double-vortex flow regime (e.g., pollutant dispersion in narrow canyons [25,26]) may not be applicable at full-scale canyons. Therefore, we should revisit the applicability of previous studies on narrow canyons and be cautious when generalizing the results from reduced-scale experiments to full-scale built environments.

IV. Conclusions

The critical Reynolds number (*Re*) for *Re*-independent flows in urban street canyon is often taken to be 10,000. Using validated CFD models, we show that this critical *Re* is not applicable for narrow canyons with height-to-width aspect ratio of 2.0. In addition, narrow canyons are often understood to exhibit the double-vortex flow regime. We show that this regime only exists at relatively low *Re* (< 28,000). At sufficiently high *Re* (> 57,000), only one major vortex is observed, consistent with full-scale field measurement [19]. This finding changes the common understanding of flows in narrow canyons, where multiple vortices are expected.

References

[1] C. Yuan, E. Ng, L.K. Norford, “Improving air quality in high-density cities by understanding the relationship between air pollutant dispersion and urban morphologies,” Build. Environ. 71 (2014), pp. 245–258.

[2] L.W. Chew, L.K. Norford, “Pedestrian-level wind speed enhancement in urban street canyons with void decks,” Build. Environ. 146 (2018), pp. 64–76.

[3] P. Kastner-Klein, R. Berkowicz, R. Britter, “The influence of street architecture on flow and dispersion in street canyons,” Meteorol. Atmospheric Phys. 87 (2004), pp. 121–131.

[4] A.A. Aliabadi, E.S. Krayenhoff, N. Nazarian, L.W. Chew, P.R. Armstrong, A. Afshari, L.K. Norford, “Effects of Roof-Edge Roughness on Air Temperature and Pollutant Concentration in Urban Canyons,” Bound.-Layer Meteorol. 164 (2017), pp. 1–31.

[5] R. Britter, S. Hanna, “Flow and dispersion in urban areas,” Annu. Rev. Fluid Mech. 35 (2003), pp. 469–496.

[6] T. Oke, Boundary layer climates, 2nd edition, Methuen, London and New York, 1987, pp. 267.

[7] X.-X. Li, C.-H. Liu, D.Y. Leung, K. Lam, “Recent progress in CFD modelling of wind field and pollutant transport in street canyons,” Atmos. Environ. 40 (2006), pp. 5640–5658.

[8] F. Caton, R.E. Britter, S. Dalziel, “Dispersion mechanisms in a street canyon,” Atmos. Environ. 37 (2003), pp. 693–702.

[9] F. Gerdes, D. Olivari, “Analysis of pollutant dispersion in an urban street canyon,” J. Wind Eng. Ind. Aerodyn. 82 (1999), pp. 105–124.

[10] J.-J. Baik, R.-S. Park, H.-Y. Chun, J.-J. Kim, “A laboratory model of urban street-canyon flows,” J. Appl. Meteorol. 39 (2000), pp. 1592–1600.

[11] X.-X. Li, D.Y. Leung, C.-H. Liu, K. Lam, “Physical modeling of flow field inside urban street canyons,” J. Appl. Meteorol. Climatol. 47 (2008), pp. 2058–2067.

[12] A. Kovar-Panskus, L. Moulinneuf, E. Savory, A. Abdelqari, J.-F. Sini, J.-M. Rosant, A. Robins, N. Toy, “A wind tunnel investigation of the influence of solar-induced wall-heating on the flow regime within a simulated urban street canyon,” Water Air Soil Pollut. Focus. 2 (2002), pp. 555–571.

[13] R.N. Meroney, M. Pavageau, S. Rafailidis, M. Schatzmann, “Study of line source characteristics for 2-D physical modelling of pollutant

dispersion in street canyons," J. Wind Eng. Ind. Aerodyn. 62 (1996), pp. 37–56.
[14] M.J. Brown, R.E. Lawson, D.S. DeCroix, R.L. Lee, "Mean flow and turbulence measurements around a 2-D array of buildings in a wind tunnel," in: 11th Jt. AMSAWMA Conf. Appl. Air Pollut. Meteorol. Long Beach CA, 2000.
[15] Y. Nakamura, T.R. Oke, "Wind, temperature and stability conditions in an east-west oriented urban canyon," Atmospheric Environ. 1967. 22 (1988), pp. 2691–2700.
[16] I. Eliasson, B. Offerle, C. Grimmond, S. Lindqvist, "Wind fields and turbulence statistics in an urban street canyon," Atmos. Environ. 40 (2006), pp. 1–16.
[17] M. Santamouris, N. Papanikolaou, I. Koronakis, I. Livada, D. Asimakopoulos, "Thermal and air flow characteristics in a deep pedestrian canyon under hot weather conditions," Atmos. Environ. 33 (1999), pp. 4503–4521.
[18] X.-X. Li, C.-H. Liu, D.Y. Leung, "Development of a k–ε model for the determination of air exchange rates for street canyons," Atmos. Environ. 39 (2005), pp. 7285–7296.
[19] W.H. Snyder, Guideline for fluid modeling of atmospheric diffusion, Environmental Protection Agency, Research Triangle Park, NC (USA), 1981.
[20] L.W. Chew, A.A. Aliabadi, L.K. Norford, "Flows across high aspect ratio street canyons: Reynolds number independence revisited," Environ. Fluid Mech. 18 (2018), pp. 1275–1291.
[21] ANSYS Inc, ANSYS FLUENT User's Guide Release 14.0, (2011).
[22] L.W. Chew, N. Nazarian, L. Norford, "Pedestrian-level urban wind flow enhancement with wind catchers," Atmosphere. 8 (2017), pp. 159.
[23] S. Hanna, J. Chang, "Acceptance criteria for urban dispersion model evaluation," Meteorol. Atmospheric Phys. 116 (2012), pp. 133–146.
[24] A.A. Aliabadi, Theory and applications of turbulence: A fundamental approach for scientists and engineers, Amir A. Aliabadi Publications, Guelph, Ontario, Canada, 2018, pp. 168.
[25] J. Zhong, X.-M. Cai, W.J. Bloss, "Large eddy simulation of reactive pollutants in a deep urban street canyon: Coupling dynamics with O3-NOx-VOC chemistry," Environ. Pollut. 224 (2017), pp. 171–184.
[26] X.-X. Li, C.-H. Liu, D.Y. Leung, "Large-eddy simulation of flow and pollutant dispersion in high-aspect-ratio urban street canyons with wall model," Bound.-Layer Meteorol. 129 (2008), pp. 249–268.